Published January 4, 2016

Cortical PAR polarity proteins promote robust cytokinesis during asymmetric cell division

Shawn N. Jordan,[1] Tim Davies,[1]* Yelena Zhuravlev,[1,2]* Julien Dumont,[3]** Mimi Shirasu-Hiza,[2]** and Julie C. Canman[1]

[1]Department of Pathology and Cell Biology and [2]Department of Genetics and Development, Columbia University, New York, NY 10032
[3]Institut Jacques Monod, Centre National de la Recherche Scientifique, Unites Mixtes de Recherche 7592, Universite Paris Diderot, Sorbonne Paris Cité, 75205 Paris, France

Cytokinesis, the physical division of one cell into two, is thought to be fundamentally similar in most animal cell divisions and driven by the constriction of a contractile ring positioned and controlled solely by the mitotic spindle. During asymmetric cell divisions, the core polarity machinery (partitioning defective [PAR] proteins) controls the unequal inheritance of key cell fate determinants. Here, we show that in asymmetrically dividing *Caenorhabditis elegans* embryos, the cortical PAR proteins (including the small guanosine triphosphatase CDC-42) have an active role in regulating recruitment of a critical component of the contractile ring, filamentous actin (F-actin). We found that the cortical PAR proteins are required for the retention of anillin and septin in the anterior pole, which are cytokinesis proteins that our genetic data suggest act as inhibitors of F-actin at the contractile ring. Collectively, our results suggest that the cortical PAR proteins coordinate the establishment of cell polarity with the physical process of cytokinesis during asymmetric cell division to ensure the fidelity of daughter cell formation.

Introduction

Cytokinesis, the physical division of one cell into two, occurs trillions of times from fertilization to death, and division failures can have significant consequences, including miscarriage, neurological dysfunction, immunological defects, and cancer (Lacroix and Maddox, 2012; Tormos et al., 2015). Cytokinesis is driven by the constriction of a contractile ring composed of formin-nucleated F-actin and the motor myosin-II, which is primarily positioned and controlled by the mitotic spindle (Green et al., 2012). Divisions in which the daughter cells inherit equal cytoplasmic and cortical components, and thus the same cell fate and size, are referred to as symmetric. In contrast, many cell divisions during embryogenesis and in adult stem cells are asymmetric, resulting in daughter cells with different cell fates and/or cell sizes (Williams and Fuchs, 2013). In metazoans, asymmetric cell division requires G protein–coupled receptors and the partitioning defective (PAR) proteins. The PAR proteins are a conserved set of proteins that segregate to opposing poles of the cell during asymmetric cell division and control the unequal inheritance of cytoplasmic and cortical factors (Macara, 2004; Suzuki and Ohno, 2006; Motegi and Seydoux, 2013).

The *Caenorhabditis elegans* single-cell zygote has been a seminal system for understanding the molecular regulation of anterior-posterior (A-P) cell polarity and the PAR proteins (Kemphues et al., 1988). In this system, opposing cortical anterior and posterior PAR (aPAR and pPAR, respectively) domains are formed via two genetically and temporally distinct phases: polarity establishment and polarity maintenance (Cuenca et al., 2003). During polarity establishment, the core cortical aPAR proteins (including the scaffolding proteins PAR-3 and PAR-6, the atypical protein kinase PKC-3, and the small GTPase CDC-42) and the core pPAR PAR-2 (a RING finger– and nucleoside triphosphatase–containing protein) are targeted to opposite sides of the cell via anteriorly directed actomyosin-based cortical flows (Hird and White, 1993; Cheeks et al., 2004; Munro et al., 2004). During polarity maintenance, the aPAR proteins and pPAR proteins remain on opposing sides of the cell cortex forming a distinct A-P boundary near the cell equator via mutual inhibition (for extensive reviews of PAR proteins, see Hoege and Hyman, 2013; Motegi and Seydoux, 2013; Rose and Gönczy, 2014).

A role for the cortical PAR proteins in cytokinesis was previously thought to be indirect by controlling spindle length and position (Dechant and Glotzer, 2003). However, emerging evidence suggests that cell polarity has a more active role in cytokinesis, though the underlying molecular mechanisms remain elusive. Perturbations in asymmetrically dividing *Drosophila melanogaster* neuroblasts revealed that spindle-independent contractile rings can form in association with a G protein–coupled receptor–promoted polarized cap of myosin-II (Caber-

*T. Davies and Y. Zhuravlev contributed equally to this paper.

**J. Dumont and M. Shirasu-Hiza contributed equally to this paper.

Correspondence to Julie C. Canman: jcc2210@cumc.columbia.edu

Abbreviations used in this paper: A-P, anterior-posterior; aPAR, anterior PAR; PAR, partitioning defective; pPAR, posterior PAR; ts, temperature sensitive.

Supplemental Material can be found at:
http://jcb.rupress.org/content/suppl/2015/12/31/jcb.201510063.DC1.html
http://jcb.rupress.org/content/suppl/2016/01/04/jcb.201510063.DC2.html
Original image data can be found at:
http://jcb-dataviewer.rupress.org/jcb/browse/11755

The Rockefeller University Press $30.00
J. Cell Biol. Vol. 212 No. 1 39–49
www.jcb.org/cgi/doi/10.1083/jcb.201510063

Published January 4, 2016

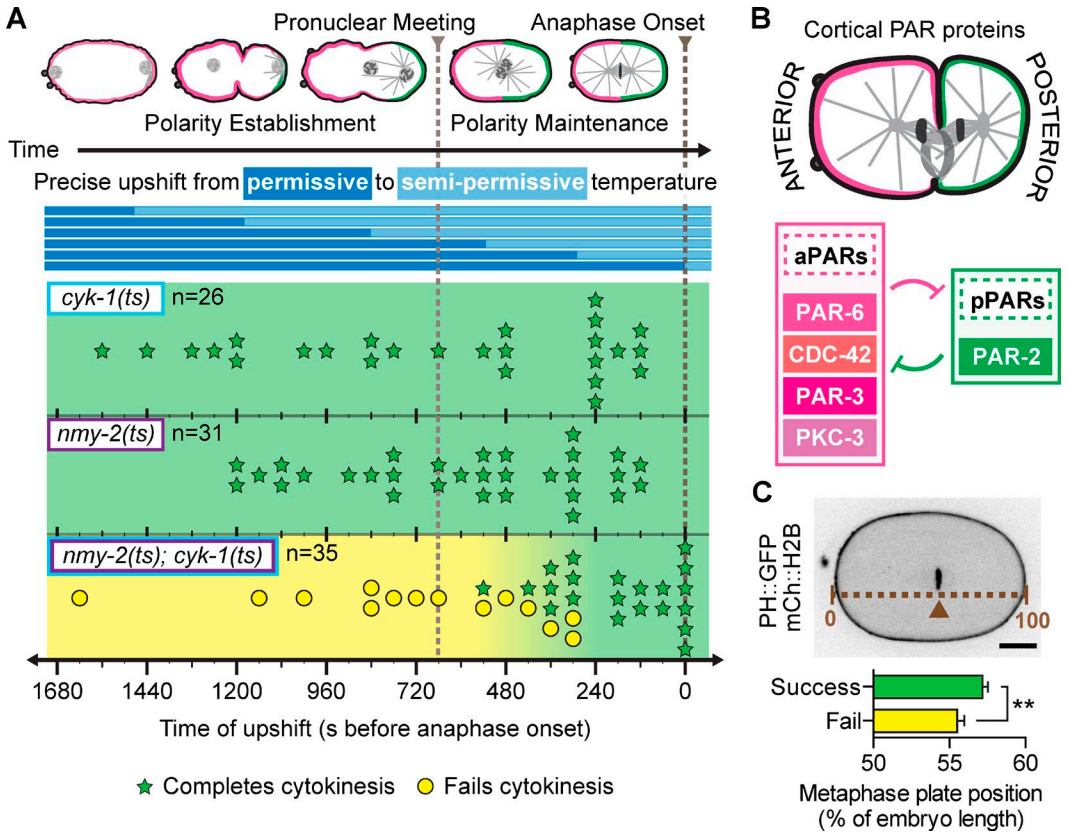

Figure 1. **Polarity establishment supports robust cytokinesis.** (A) Experimental protocol and rapid temperature upshift results. Each symbol (star or circle) represents a single embryo plotted at the time of upshift. (B) Schematic of cortical PAR protein localization during asymmetric cell division. (C) The metaphase plate (arrowhead) in *myosin-II(ts);formin(ts)* embryos that complete cytokinesis (n = 21) is positioned more asymmetrically than in those that fail (n = 14; mean ± SD). **, P < 0.005. Bar, 10 µm. *cyk-1* = *formin*; *nmy-2* = *myosin-II*.

nard et al., 2010). In *C. elegans*, depletion of PAR-2 enhances contractile ring constriction defects caused by compromised spindle signaling (Dechant and Glotzer, 2003; Verbrugghe and White, 2007). Moreover, both the aPAR and pPAR proteins "track" with the contractile ring during cytokinesis (Schenk et al., 2010; Pittman and Skop, 2012).

Here, we show that in the asymmetrically dividing *C. elegans* zygote, cortical A-P polarity protects the cell against cytokinesis failure in the presence of a weakened actomyosin contractile ring. We demonstrate that both the core cortical aPAR (including CDC-42) and pPAR proteins are required for proper F-actin levels at the contractile ring and restrict the localization of two actomyosin-binding and cross-linking proteins, anillin^{ANI-1} and septin^{UNC-59}. We found that anillin and septin have unexpected inhibitory roles in F-actin accumulation at the contractile ring. Thus, we present a model in which cortical PAR proteins protect cytokinesis during asymmetric cell division independent of mitotic spindle length by promoting the anterior retention of anillin and septin away from the contractile ring, thus allowing for robust F-actin accumulation and ring constriction.

Results and discussion

A synergistic interaction between formin and myosin-II mutants during polarity establishment leads to cytokinesis failure

The F-actin nucleator diaphanous-like formin^{CYK-1} (hereafter formin) and the motor myosin-II^{NMY-2} (hereafter myosin-II) are known to be critical for cytokinesis (Fig. S1 A; Swan et al., 1998; Shelton et al., 1999; Severson et al., 2002). Using fast-acting temperature-sensitive (ts) mutants with point mutations in the formin dimerization (FH2) domain, required for actin polymerization, and in the myosin-II neck (S2) domain, required for dimerization and head coupling (Liu et al., 2010; Davies et al., 2014), we found that formin and myosin-II are synergistic. At semipermissive temperatures, where the proteins are perturbed but functional enough to allow cytokinesis (Fig. S1 A), 100% of *myosin-II(ts)* and *formin(ts)* single mutant embryos divided successfully, whereas ~40% of *myosin-II(ts);formin(ts)* double mutant embryos failed to divide, suggesting a synthetic cytokinesis defect (14/35 embryos; Figs. 1 A and S1 B).

To identify the time of requirement for this synthetic interaction, we used a fluidic device (Davies et al., 2014) to rapidly upshift (<20 s) *myosin-II(ts);formin(ts)* double mutant embryos to this semipermissive temperature at precise time points during cell division. Unexpectedly, we found that this synthetic interaction and cytokinesis failure occur only when myosin-II and formin are both disrupted well before cytokinesis, during establishment and maintenance of A-P polarity (Fig. 1 A). Upshift during polarity establishment caused cytokinesis failure in all *myosin-II(ts);formin(ts)* double mutants (7/7). Upshift during polarity maintenance caused an intermediate failure rate (7/22), with all failures seen in earlier upshifts. Upshift after the polarity maintenance phase did not cause cytokinesis failure in any double mutants (0/6). Thus, the synthetic effect is strictly limited to the time period correlated with polarity establishment and maintenance and not during cytokinesis directly.

Published January 4, 2016

Polarity establishment is dependent on myosin-II but independent of formin activity (Fig. S1 C; Cuenca et al., 2003; Munro et al., 2004; Velarde et al., 2007; Liu et al., 2010). Thus, we hypothesized that synthetic cytokinesis failure is caused by myosin-II function as a polarity protein, synergizing with an independent formin function. Consistent with this hypothesis, we found that the *myosin-II(ts);formin(ts)* double mutant embryos that failed in cytokinesis were also less polarized, with more centrally located metaphase plates relative to those that succeeded in cytokinesis (Fig. 1 C). It is unlikely that this early interaction represents a delay in functional inhibition, as both ts mutants are very fast acting and show a full loss of function phenotype within seconds upon upshift to restrictive temperature (Davies et al., 2014). Furthermore, cytokinesis completed successfully when embryos were upshifted to restrictive temperature during polarity establishment then downshifted to permissive temperature before anaphase onset (Fig. S1 D). Collectively, these results suggest that establishment of A-P polarity (very early in the cell cycle, before nuclear envelope breakdown) is required for efficient contractile ring constriction during cytokinesis, a significantly later cell cycle event.

Core cortical PAR proteins are required for cytokinesis when formin activity is weakened

Establishment of A-P polarity requires both core cortical aPAR and pPAR proteins (Figs. 1 B and 2 A). Myosin-II itself is a cortical aPAR, required for polarity establishment and maintenance and localizing to the anterior cortex (Guo and Kemphues, 1996; Cuenca et al., 2003; Liu et al., 2010). To directly test a role for A-P polarity in cytokinesis, we RNAi depleted five different cortical PAR proteins in either *formin(ts)* or *myosin-II(ts)* mutants to assess these synthetic interactions for cytokinesis function. Depletion of the aPAR proteins (PAR-6, PAR-3, PKC-3, or CDC-42) or pPAR (PAR-2) caused cytokinesis failure in *formin(ts)* embryos at semipermissive temperature, with little to no contractile ring constriction (Figs. 2 B and S3 B). In contrast, PAR depletion slowed but did not block cytokinesis in *myosin-II(ts)* embryos at semipermissive temperature (Figs. 2 C and S3 B). Depletion of each PAR alone, in the absence of another mutation, did not cause cytokinesis failure (Fig. 2, B and C; and Fig. S3 B), consistent with a synthetic effect. Successful PAR depletion was confirmed by four hallmarks of loss of polarity (see Materials and methods sections RNAi and Image analysis; Fig. 2 A; Fig. S2, A–D; and Fig. S3 A). These data suggest that myosin-II and the core cortical PAR proteins act together during A-P polarity establishment to regulate cytokinesis synergistically with formin. That is, the cortical PAR and formin pathways each contribute to cytokinesis, and weakening either one alone is not sufficient to cause cytokinesis failure, but weakening both pathways prevents cytokinesis.

Why are both aPAR proteins and pPAR proteins required for robust cytokinesis when formin activity is weakened? One possibility is that cytokinesis in asymmetrically dividing cells requires opposing cortical PAR domains or the A-P polarity boundary, maintained by mutual aPAR and pPAR exclusion. If so, the A-P polarity boundary might act as a special site that facilitates contractile ring assembly and constriction. Indeed, we found that furrow initiation occurred near the A-P polarity boundary (where PAR-6 levels are decreasing and PAR-2 levels begin to increase), suggesting a possible association between the A-P boundary and the initial site of contractile ring assembly (Fig. 2, D and E).

Cytoplasmic polarity and spindle length are not key regulators of cytokinesis when formin activity is compromised

To identify factors downstream of the core cortical PAR proteins during cytokinesis, we first examined PAR-1 and PAR-4, which mediate the asymmetric inheritance of key cytoplasmic components (e.g., RNA granules) and differential daughter cell cycle timing (Fig. S2, E and F) but are dispensable for cortical A-P polarity in the one-cell embryo (Fig. 3 A). PAR-1 localizes to the posterior cell cortex (Boyd et al., 1996); PAR-4 localizes uniformly on the cortex (Watts et al., 2000) and has been shown to regulate myosin-II during cytokinesis (Chartier et al., 2011; Pacquelet et al., 2015). We found that depletion of either PAR-1 or PAR-4, alone or in combination with the *formin(ts)* or *myosin-II(ts)* mutation, did not affect cytokinesis (Fig. 3 B), suggesting that this role in cytokinesis is specific to the core cortical PAR proteins.

It was previously suggested that cortical PAR proteins indirectly regulate cytokinesis by increasing spindle length and astral separation (Dechant and Glotzer, 2003; Lewellyn et al., 2010). We did not find any correlation between reduced spindle length and the success or failure of cytokinesis after cortical PAR depletion (Fig. 3 C). Although PAR-2 depletion decreased spindle length and caused cytokinesis failure in *formin(ts)* mutants, PAR-6 depletion increased spindle length and also caused cytokinesis failure (Fig. 3 C). Similarly, although PAR-2 depletion in *myosin-II(ts)* mutants led to very short spindles, cytokinesis did not fail with either PAR-2 or PAR-6 depletion in this mutant (Fig. 3 C). Thus, the effects of core cortical PAR proteins on cytokinesis in this system are not caused by downstream effects on cytoplasmic factors or reduced spindle length.

The core cortical PAR proteins are required for normal F-actin accumulation in the contractile ring

Because the myosin-II–cortical PAR pathway shows a synthetic interaction with the formin pathway during cytokinesis and a major function of formin is actin polymerization, we next tested whether the core cortical PAR proteins regulate F-actin levels in the contractile ring, using GFP-tagged reporters to monitor F-actin and myosin-II (Fig. 3 D). Depletion of either PAR-6 or PAR-2 alone led to a 30% and 27% reduction, respectively, in F-actin levels at the contractile ring (Fig. 3 E), consistent with their synthetic cytokinesis failure phenotypes. Effects on myosin-II levels were inconsistent between PAR-6 and PAR-2, as depletion of PAR-6 led to a 31% decrease and PAR-2 led to a 48% increase in myosin-II levels in the contractile ring (Fig. 3 F), as expected from their opposing effects on global cortical myosin-II levels (Munro et al., 2004). These data suggest that both the cortical aPAR and pPAR proteins promote normal F-actin levels at the contractile ring in asymmetrically dividing cells and that this function is synthetic with compromised formin activity during cytokinesis.

The cortical PAR proteins mediate the anterior retention of anillin and septin and restrict their targeting to the contractile ring

How do the PAR proteins regulate F-actin levels at the contractile ring? The anterior of the early embryo is enriched for several actomyosin-binding and regulatory proteins (Munro et al., 2004). Starting from a list of genes that genetically interact

Published January 4, 2016

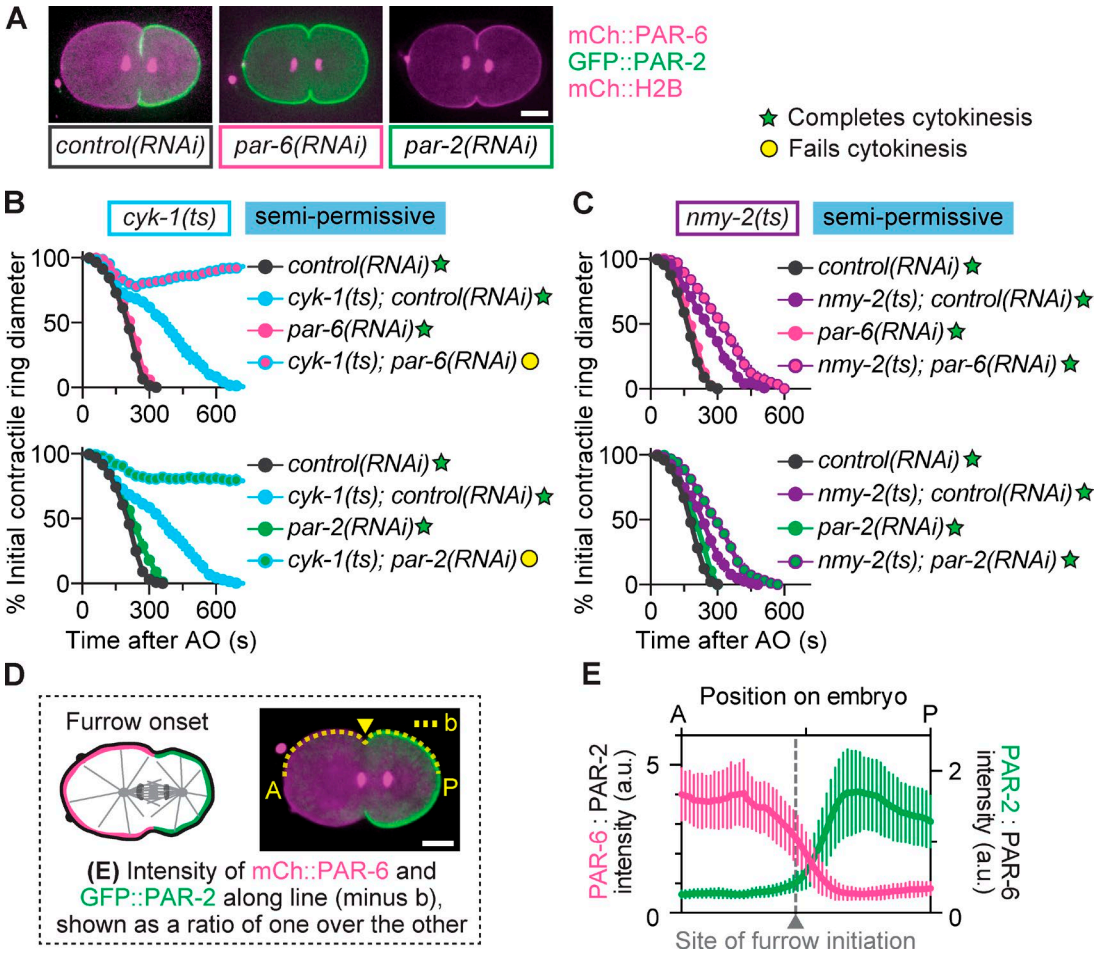

Figure 2. **PAR proteins protect against cytokinesis failure when formin activity is reduced.** (A) RNAi depletion of cortical PAR proteins disrupts A-P polarity. (B and C) Depletion of cortical PAR proteins leads to cytokinesis failure in *formin(ts)* (B) but not *myosin-II(ts)* mutant embryos (C) at semipermissive temperature (n = 10, all conditions; mean ± SEM). (D) Schematic of cortical line scan used for analysis in E. The arrowhead points to the site of initial furrow formation. (E) The A-P polarity boundary, where PAR-2 levels start to increase relative to PAR-6 levels, coincides with the site of furrow onset (gray line; n = 10; mean ± SD). Bars, 10 µm. AO, anaphase onset; a.u., arbitrary units; b, background. *cyk-1* = *formin*; *nmy-2* = *myosin-II*.

with the cortical PAR proteins (Fievet et al., 2013), we next identified asymmetric (anterior) enrichment of two actomyosin-binding and cross-linking proteins implicated in cytokinesis: septin^{UNC-59} (hereafter septin) and anillin^{ANI-1} (hereafter anillin; Fig. 4 A–C; and Fig. S3, C and D; Oegema et al., 2000; Field et al., 2005; Straight et al., 2005; Maddox et al., 2007; Bridges and Gladfelter, 2015). We found that this anterior localization of septin and anillin is dependent on the cortical PAR proteins (Fig. 4, A–C; and Fig. S3, C and D). That is, depletion of PAR-6 or PAR-2 led to a decrease in anterior enrichment and increase in posterior enrichment of GFP::septin and GFP ::anillin during metaphase (Fig. 4, A–C; and Fig. S3, C and D). During furrow onset, septin and anillin remained polarized in control embryos (Fig. S3, E and F). In contrast, PAR-6 or PAR-2 depletion decreased the polarization of septin and anillin and increased their levels at the contractile ring both at furrow onset (Fig. S3, E and F) and during ring constriction (37% and 42% increases in septin and 29% and 21% increases in anillin after PAR-6 and PAR-2 depletion, respectively; Fig. 4, A, D, and E). Importantly, depletion of neither septin nor anillin disrupted A-P polarity (by PAR-6 and PAR-2 distribution), suggesting that these proteins are downstream of the cortical PAR proteins (Fig. 4 F). Thus, the core cortical PAR proteins are required for the asymmetric anterior localization of both septin and anillin (Fig. 4 G) and to restrict their accumulation at the contractile ring during cytokinesis.

Septin and anillin negatively regulate F-actin levels in the contractile ring

Because we found that the core cortical PAR proteins modulate F-actin levels at the contractile ring and are also required to spatially restrict septin and anillin, we next tested whether septin and anillin also modulate F-actin and/or myosin-II levels in the contractile ring. Unexpectedly, RNAi-mediated depletion of either septin or anillin led to increased F-actin levels in the contractile ring (20% and 19%, respectively; Fig. 5, A and B), suggesting that these two proteins inhibit F-actin accumulation. As previously published, depletion of septin or anillin led to a 24% increase or no change (respectively) in myosin-II levels in the ring (Fig. 5, A and C; Maddox et al., 2007; Lewellyn et al., 2011). These results demonstrate that PAR-6 and PAR-2 have opposite effects on spindle length and myosin-II localization but similar effects on F-actin, septin, and anillin levels in the contractile ring during cytokinesis. These results further suggest that septin and anillin function as negative regulators of F-actin accumulation at the contrac-

Published January 4, 2016

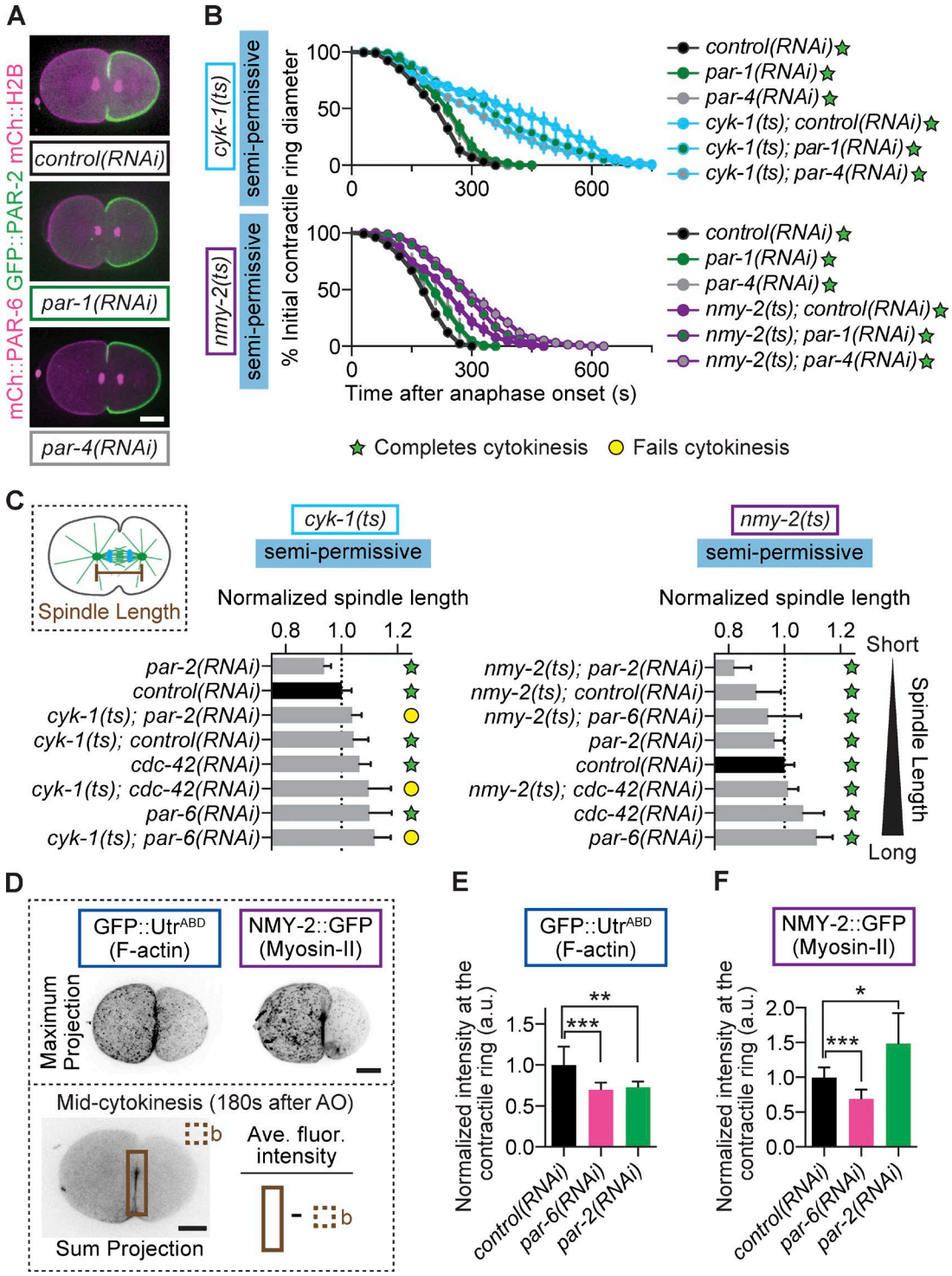

Figure 3. **The cortical PAR proteins regulate F-actin in the contractile ring during cytokinesis and not via downstream PAR proteins or spindle length.** (A) Depletion of neither PAR-1 nor PAR-4 disrupts A-P cortical polarity. (B) RNAi depletion of PAR-1 or PAR-4 does not lead to cytokinesis failure in *formin(ts)* or *myosin-II(ts)* mutant embryos at semipermissive temperatures (n = 10, all conditions; mean ± SEM). (C) Spindle lengths for all conditions arranged from shortest to longest at the *formin(ts)* or *myosin-II(ts)* semipermissive temperature. Error bars represent SD. (D) Schematic of region and formula used for analysis shown in E and F. The boxed area represents the region used for measurements in the contractile ring. (E) Depletion of PAR-6 or PAR-2 reduces F-actin levels in the contractile ring relative to controls (*control(RNAi)* n = 13, *par-6(RNAi)* n = 7, *par-2(RNAi)* n = 7; mean ± SD). (F) Depletion of PAR-6 or PAR-2 has opposing effects on myosin-II levels in the contractile ring, relative to controls (*control(RNAi)* n = 13, *par-6(RNAi)* n = 7, *par-2(RNAi)* n = 7; mean ± SD). *, $P < 0.05$; **, $P < 0.005$; ***, $P < 0.0005$. Bars, 10 µm. AO, anaphase onset; b, background. *cyk-1* = *formin*; *nmy-2* = *myosin-II*.

tile ring during cytokinesis, and their PAR-dependent anterior polar retention allows proper F-actin accumulation at the ring during asymmetric cell division.

Depletion of septin and anillin suppresses cytokinesis failure in formin mutants with and without the cortical PAR proteins

Published January 4, 2016

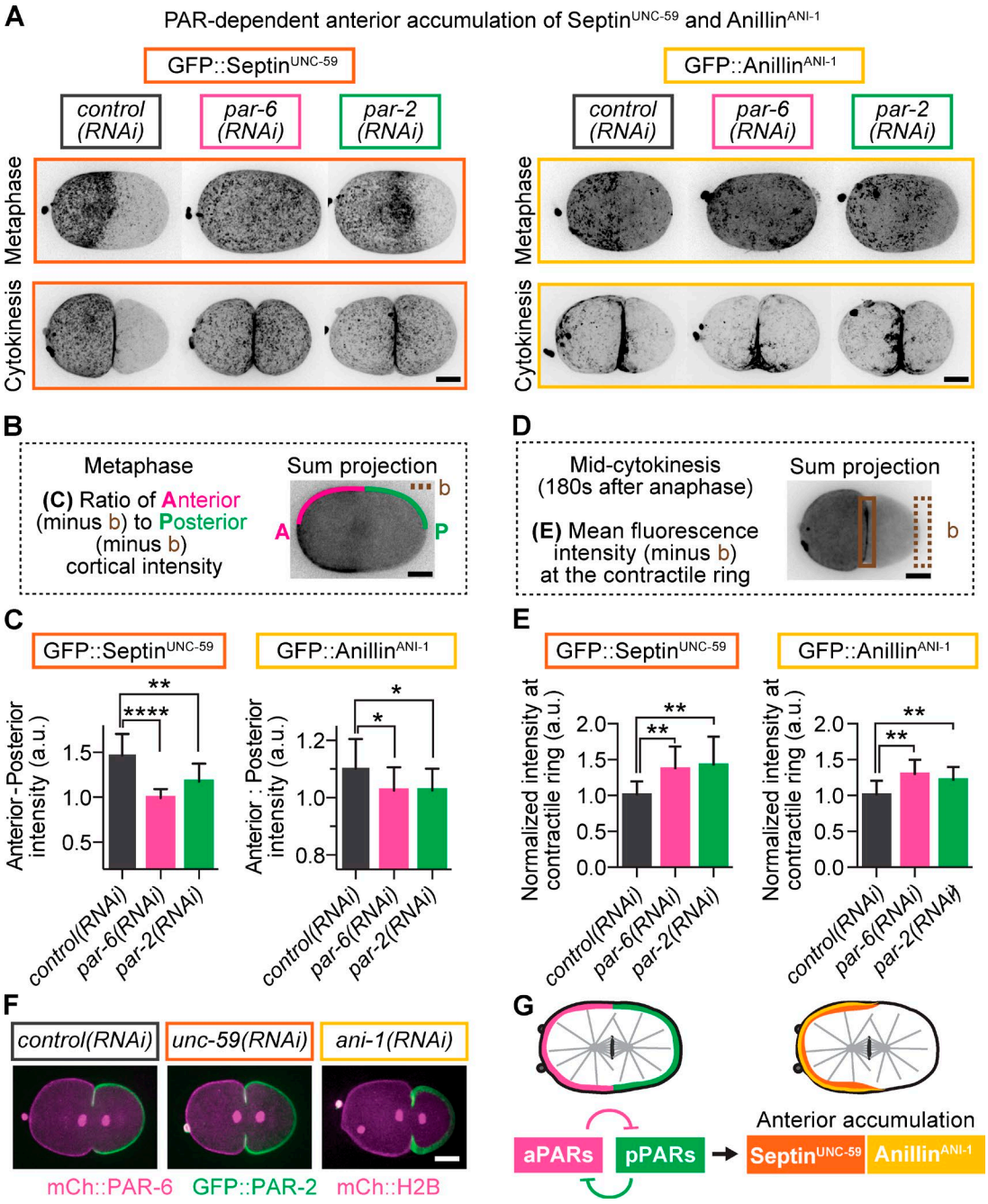

Figure 4. **PAR proteins are required to retain septin and anillin in the cell anterior away from the contractile ring.** (A) Representative images of maximum projections of GFP::septin^{UNC-59} and GFP::anillin^{ANI-1} at metaphase and during cytokinesis, with and without A-P polarity. (B) Schematic of anterior and posterior cortical line scans used for analysis shown in C. (C) Ratio of anterior to posterior cortical fluorescence of septin and anillin with and without PAR-6 and PAR-2 depletion ($n \geq 10$, all conditions; mean ± SD). (D) Schematic of region and formula used for analysis shown in E. The boxed area represents the region used for measurement in the contractile ring. (E) Septin and anillin levels in the contractile ring increase a disruption of A-P polarity. Error bars represent SD. (F) Depletion of septin or anillin does not disrupt A-P polarity. (G) Anterior enrichment of septin and anillin is PAR dependent but not vice versa. *, $P < 0.05$; **, $P < 0.005$; ****, $P < 0.0001$. Bars, 10 µm. a.u., arbitrary units; b, background. *ani-1* = *anillin*; *unc-59* = *septin*.

We finally predicted that if loss of cortical PAR proteins enhances cytokinesis failure in formin mutants by increasing the levels of septin and anillin in the contractile ring, then depletion of septin and/or anillin should rescue cytokinesis failure in *formin(ts)* mutants lacking A-P polarity. Consistent with this prediction, we found that depletion of septin completely rescued cytokinesis failure in *formin(ts);par-6(RNAi)* and *formin(ts);par-2(RNAi)* zygotes, even at semirestrictive temperature when *formin(ts)* mutants alone failed in cytokinesis (Figs. 5 D and S1 A). These results suggest that the synthetic interaction between loss of formin activity and loss of PAR proteins is dependent on septin. Thus, the major contribution of the cortical PAR proteins to cytokinesis may be to inhibit septin because in the absence of septin, the PAR proteins are dispensable. Indeed, depletion of septin or anillin rescues cytokinesis failure in *formin(ts)* mutants but not in *myosin-II(ts)* mutants (Fig. 5, E and F). Although depletion

Published January 4, 2016

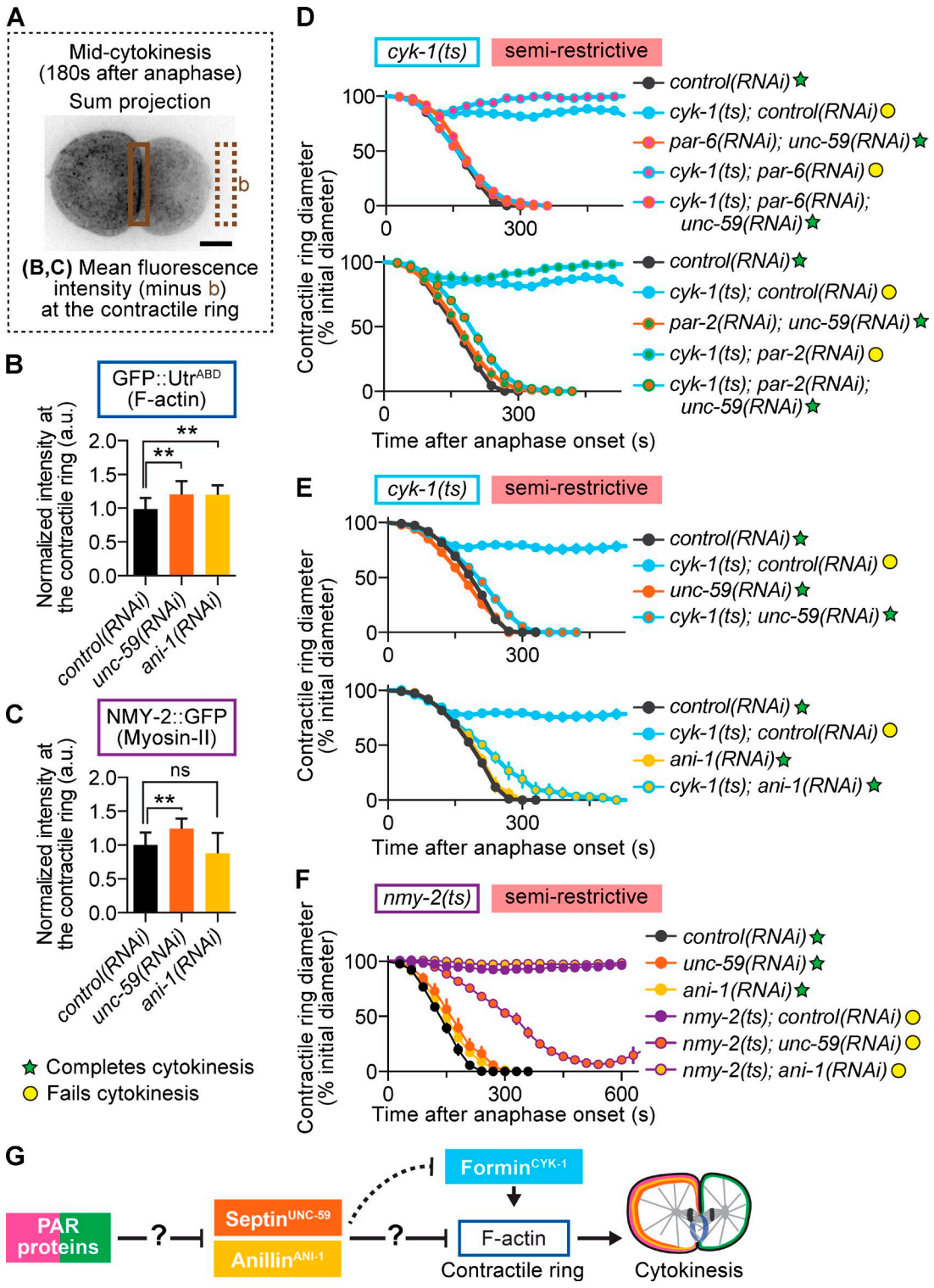

Figure 5. **Septin and anillin restrict contractile ring F-actin levels and negatively regulate cytokinesis.** (A) Schematic of region and formula used for analysis shown in B and C. The boxed area represents the region used for measurement in the contractile ring. (B and C) Depletion of septin and anillin increased F-actin levels in the contractile ring (B), whereas only septin depletion increased myosin-II levels in the ring (C; $n \geq 10$, all conditions; mean ± SD). **, $P < 0.005$; ns, not significant. (D) Depletion of septin suppresses cytokinesis failure in *formin(ts)* mutant embryos at semirestrictive temperature, even when A-P polarity is simultaneously disrupted (*control(RNAi)* $n = 9$, *cyk-1(ts);control(RNAi)* $n = 11$, *par-6(RNAi);unc-59(RNAi)* $n = 11$, *cyk-1(ts);par-6(RNAi)* $n = 3$, *cyk-1(ts);par-6(RNAi);unc-59(RNAi)* $n = 12$, *par-2(RNAi);unc-59(RNAi)* $n = 10$, *cyk-1(ts);par-2(RNAi)* $n = 4$, *cyk-1(ts);par-2(RNAi);unc-59(RNAi)* $n = 12$; mean ± SEM). (E) Depletion of septin and anillin suppresses cytokinesis failure in *formin(ts)* mutant embryos at semirestrictive temperature ($n = 10$, all conditions; mean ± SEM). (F) RNAi-mediated depletion of neither anillin nor septin suppresses cytokinesis failure in *myosin-II(ts)* mutant embryos at semirestrictive temperature ($n \geq 8$, all conditions; mean ± SEM). (G) In our genetic model, PAR proteins inhibit septin and anillin localization in the contractile ring by promoting their anterior retention. This prevents septin and anillin from inhibiting F-actin and thereby promotes robust cytokinesis. The question marks reflect that the mechanism of action, whether via a direct interaction or other intermediate players in the pathway, is unknown. Bar, 10 µm. a.u., arbitrary units; b, background. *cyk-1* = *formin*; *nmy-2* = *myosin-II*; *ani-1* = *anillin*; *unc-59* = *septin*.

Published January 4, 2016

of septin (but not anillin) led to increased contractile ring constriction in *myosin-II(ts)* embryos at semirestrictive temperature, cytokinesis ultimately failed in 100% of embryos (Fig. 5 F). This is consistent with the increase in contractile ring myosin-II levels observed after septin (but not anillin) depletion (Fig. 5 C). Collectively, our results suggest a model in which opposing cortical aPAR and pPAR proteins promote robust cytokinesis during asymmetric cell division by mediating the localization of septin and anillin to the cell anterior (Fig. 5 G). Further experiments will be necessary to determine whether this is a direct or indirect effect.

Although we were initially surprised by the inhibitory role for anillin and septin during cytokinesis, there is little consensus for a positive regulatory role for these proteins in cell division. Anillin homologues are not required for contractile ring assembly and constriction in many systems, including budding yeast (Norden et al., 2006), fission yeast (Chang et al., 1996), many *C. elegans* cell types (Maddox et al., 2007), some cells in *Drosophila* (Field et al., 2005; O'Farrell and Kylsten, 2008), zebrafish ganglion cell progenitors (Paolini et al., 2015), and even HeLa cells, in which loss of anillin causes cytokinesis failure in only 15–50% of cells (Straight et al., 2005; Piekny and Glotzer, 2008). The septins, originally identified in the asymmetrically dividing budding yeast, are required in that system for mother–daughter cell separation but not for actomyosin contractile ring constriction (Wloka et al., 2011). Septins are also dispensable for most cytokinetic events in fission yeast (Wu et al., 2010), worms (Nguyen et al., 2000; Maddox et al., 2007), some *Drosophila* cell types (Field et al., 2008), and in many human cell types (Menon and Gaestel, 2015). In fact, ring constriction is faster without the septins in some systems (Lewellyn et al., 2011; Wloka et al., 2011). Anillin and septin have also both been implicated in regulating the asymmetry of contractile ring constriction within the division plane (Maddox et al., 2007). This role is quite different than the PAR-dependent asymmetry in daughter cell fate and size that we describe here. Our data suggest that, at least in asymmetrically dividing *C. elegans* embryos, anillin and septin function as negative regulators of contractile ring assembly and constriction, perhaps because of their ability to cross-link F-actin and/or myosin-II and thus increase drag or filament severing or reduce filament turnover.

Two classic hallmarks of cancer progression are the loss of cell polarity and defects in cytokinesis (Ganem et al., 2007; Davoli and de Lange, 2011; Halaoui and McCaffrey, 2015). Here, we demonstrate that during asymmetric cell division the PAR proteins actively promote robust contractile ring constriction during cytokinesis. This regulation might help protect against division errors and protect the fidelity of critical asymmetric cell divisions, such as in proliferating stem cells. Our work also suggests that the loss of cell polarity increases the incidence of cytokinesis failure and thus could be a cause, rather than an effect, of cancer development.

Materials and methods

Strain maintenance

C. elegans were maintained on standard nematode growth media plates seeded with OP50 *Escherichia coli* as previously described (Brenner, 1974). Strain names and genotypes used in this study can be found in Table S1. A. Maddox (University of North Carolina, Chapel Hill, Chapel Hill, NC) provided the strains OD159 [GFP::ANI-1] and OD26 [GFP::UNC-59], the latter of which was crossed with a strain containing the histone marker ltIs37[pAA64; pie-1/mCHERRY::his-58; unc-119 (+)] to generate JCC425. M. Glotzer (University of Chicago, Chicago, IL) provided a strain containing the F-actin marker mgSi3[tb-unc-119(+) GFP::Utrophin], which was crossed with a strain containing the histone marker ltIs37[pAA64; pie-1/mCHERRY::his-58; unc-119 (+)] to generate JCC719.

Temperature control

Control and ts strains were maintained in an incubator (Binder) at a permissive temperature (16.0 ± 0.5°C), except JCC744, JCC719, JCC541, JCC425, and OD159, which were maintained at room temperature to prevent the silencing of fluorescent reporters. Live imaging was performed in a room with homeostatic temperature control set to the desired temperature at least 1 h before the experiment. The temperature of the specimen was continuously monitored using three thermometers attached directly to the objective lens with a glue gun. Where denoted throughout the paper, room temperatures were as follows: *formin(ts)*, semipermissive temperature (18.5 ± 0.5°C); *formin(ts)*, semirestrictive temperature (23.5 ± 0.5°C); *myosin-II(ts)*, semipermissive temperature (22.0 ± 0.5°C); *myosin-II(ts)*, semirestrictive temperature (25.5 ± 0.5°C) and fully restrictive temperature (26.5 ± 0.5°C). During Therminator experiments (Fig. 1 A; and Fig. S1, B and D), the room was maintained at the *formin(ts)* semipermissive temperature (18.5 ± 0.5°C; Davies et al., 2014).

Rapid temperature shifts

Rapid temperature shifts were performed using a custom-built fluidic system called the Therminator (Bioptechs; Davies et al., 2014) with one water/isopropanol bath maintained at permissive temperature (16.0 ± 0.5°C) and a second bath at the semipermissive temperature (18.5 ± 0.5°C; Figs. 1 A and S1 B) or restrictive temperature (26.5 ± 0.5°C; Fig. S1 D). A switch mechanism determines which water bath supplies liquid for the chamber above the specimen. Forced heat convection from the flow chamber to the glass barrier directly above the specimen chamber rapidly shifts the sample temperature.

Live cell imaging

Young gravid hermaphrodites were dissected in a 16°C M9 buffer (Brenner, 1974) and mounted on a thin 2% agar pad as previously described (Gönczy et al., 1999; Davies et al., 2014). Embryos were filmed using a spinning disc confocal unit (CSU-10; Yokogawa Electric Corporation) with Borealis (Spectral Applied Research) on an inverted microscope (Ti; Nikon) with a 60× 1.4 NA oil-immersion Plan Apochromat objective with 2 × 2 binning on a charge-coupled device camera (Orca-R2; Hamamatsu Photonics). During temperature shift experiments, a 20× 0.75 NA dry objective was used. Z-sectioning was done with a Piezo-driven motorized stage (Applied Scientific Instrumentation), and focus was maintained using Perfect Focus (Nikon) before each z-series acquisition. An acousto-optic tunable filter was used to select the excitation light of two 100-mW lasers for excitation at 491 and 561 nm for eGFP and mCherry, respectively (Spectral Applied Research), and a filter wheel was used for emission wavelength selection (Sutter Instrument). The system was controlled by MetaMorph software (Molecular Devices).

A central differential interference contrast image and a through-cell fluorescent z-series were collected every 30 s to measure contractile ring dynamics (7 × 2.0-µm steps; Fig. 2, B and C; Fig. 3 B; Fig. 5, D–F; Fig. S1 A; and Fig. S3 B) or every 60 s for Therminator upshifts (5 × 2.0-

Published January 4, 2016

μm steps; Fig. 1 A; and Fig. S1, B and D) and measurement of fluorescent reporter accumulation in the cell poles and contractile ring (11 × 2.5-μm steps; Fig. 2, D and E; Fig. 3, D–F; Fig. 4, B–E; Fig. 5, A–C; and Fig. S3, C–F). 3 × 1.0-μm steps were acquired at the cell cortex for Fig. S1 C.

Image analysis

MetaMorph and ImageJ (National Institutes of Health) software were used for all data analysis. Metaphase plate positions were measured 30 s before anaphase onset. In Fig. 1 C, positions are shown relative to the A-P axis with the anterior pole being 0% and the posterior pole being 100%. In Fig. S2 (A and C), the distance between the posterior pole and the metaphase plate was subtracted from the distance between the anterior pole and the metaphase plate. Positions reflect the displacement of the metaphase plate from the cell center (0 μm).

Contractile ring diameter was measured at the cell equator from anaphase onset until, in the case of cytokinesis completion, anaphase of the subsequent cell cycle or, in the case of cytokinesis failure, the contractile ring had completely regressed and the next cell cycle began in the aneuploid cell. The ring diameter was measured as the shortest distance between the furrow tips using a fluorescent marker targeted to the plasma membrane (PH::GFP, pleckstrin homology domain; Audhya et al., 2005). For each time point, the z plane at which the ring diameter was widest was used for this measurement. Contractile ring diameter was plotted as a percentage of the initial diameter (at metaphase) as a function of time. Anaphase onset was determined using a fluorescent histone marker (mCherry::Histone2B; Audhya et al., 2007) and was set as the first time point at which distinct sister chromatids became visible.

Cortical localization of fluorescent markers (GFP::anillin^{ANI-1} and GFP::septin^{UNC-59}; Maddox et al., 2007) was measured at metaphase (one frame before anaphase onset) and furrow onset (one frame before formation of a "double membrane furrow" ∼60 s after anaphase onset). A sum projection of seven central planes was generated, and the mean fluorescence was measured along a line scan tracing the cortex from the anterior to the posterior pole. The mean fluorescence was measured outside of the cell and subtracted from the cortical fluorescence. Values along the cortical line scan were then normalized to the line mean for that cell; that is, a homogeneous cortex would have a value of 1 at all points. In Fig. 2 (D and E), the mean fluorescence of the two polarity markers (mCh::PAR-6 and GFP::PAR-2; Schonegg et al., 2007) was measured similarly but are shown as a ratio of one to the other rather than being normalized to the line mean. Fluorescence values around polar bodies were removed from line scans. Polarized accumulation of GFP::anillin^{ANI-1} and GFP::septin^{UNC-59} (Fig. 4, B and C) was calculated at metaphase as a ratio of the mean fluorescence in the anterior half to the posterior half of the embryo.

The accumulation of contractile ring markers (GFP::Utrophin^{ABD}, myosin-II^{NMY-2}::GFP, GFP::septin^{UNC-59}, and GFP::anillin^{ANI-1}; Munro et al., 2004; Burkel et al., 2007; Maddox et al., 2007; Tse et al., 2012) was measured 180 s after anaphase onset from a through-cell z-series sum projection (11 planes encompassing the entire cell). The mean fluorescence was measured in a 65-μm^2 region that encompassed the contractile ring. The mean fluorescence of an equivalent background region was measured outside of the cell and subtracted from the mean ring fluorescence. Intensities were then normalized to the contractile ring of *control(RNAi)* embryos imaged on the same day.

Daughter cell size asymmetry was measured at the time of contractile ring closure (0% initial diameter) and is shown as a ratio of the AB (anterior daughter cell) length to the P1 (posterior daughter cell) length. Cell cycle asymmetry was measured as the difference in time from anaphase onset in AB to the time of anaphase onset in P1. Spindle lengths were measured 150 s after anaphase onset using transmitted light (differential interference contrast) to visualize the spindle poles. Distances were normalized to the spindle length of controls at the same temperature.

RNAi

Exonic sequences from the desired gene were cloned into the multiple cloning site of the L4440 vector using standard cloning techniques and then transformed into HT115 *E. coli* using $CaCl_2$ transformation as previously described (Timmons et al., 2001). RNAi primers and template DNA for each gene are listed in Table S2. When available, RNAi constructs were obtained directly from the Ahringer RNAi library (Kamath and Ahringer, 2003). For double RNAi constructs (*par-6;unc-59* and *par-2;unc-59*), exonic sequences for either *par-6* or *par-2* were cloned into the multiple cloning site of pJC55 (L4440 containing *unc-59*), which was linearized via EcoRI digestion.

RNAi feeding bacteria were grown in Luria broth with ampicillin (100 μg/ml) for 8–16 h at 32°C. 300 μl of this culture was plated on RNAi plates (nematode growth media agar plates [Brenner, 1974] supplemented with 50 μg/ml ampicillin and 1 mM IPTG). These plates were allowed to dry and grow at 32°C for 24–48 h. L1 worms were plated on RNAi plates and then incubated at 16°C for 72 h before filming. Successful RNAi-mediated knockdown of PAR proteins was confirmed using four hallmarks of the loss of polarity (Bossinger and Cowan, 2012): (1) reduced spindle displacement at metaphase, (2) loss of daughter cell size asymmetry after division, (3) high embryonic lethality, and (4) mislocalized fluorescent reporters for the anterior (mCh::PAR-6) and posterior (GFP::PAR-2) domains and/or loss of cell cycle asynchrony in the AB/P1 cell divisions (Fig. S2).

Statistical analysis

Unpaired two-tailed *t* tests were conducted using Prism (GraphPad Software).

Online supplemental material

Fig. S1 shows that ts mutants allow tuning of specific protein functions that are necessary for cytokinesis. Fig. S2 shows successful RNAi-mediated knockdown of PAR proteins as confirmed by classic hallmarks of the loss of polarity. Fig. S3 shows that cortical PAR proteins regulate cytokinesis and sequester septin and anillin in the cell anterior. Table S1 contains the strain names and genotypes used in the study. Table S2 details the feeding RNAi constructs used, as well as relevant information for their construction when needed. Online supplemental material is available at http://www.jcb.org/cgi/content/full/jcb.201510063/DC1. Additional data are available in the JCB DataViewer at http://dx.doi.org/10.1083/jcb.201510063.dv.

Acknowledgments

We thank all members of the Canman, Shirasu-Hiza, and Dumont laboratories for support; Gregg Gundersen, Clare Waterman, Sriramkumar Sundaramoorthy, and Andy Kummel for critical reading; Natalia Spica, Isaiah Thomas, and Vandana Chand for laboratory assistance; Jennifer Waters for microscopy consultation; and Amy Maddox, Michael Glotzer, and the Caenorhabditis Genetics Center for worm strains.

This work is supported by grants ANR-09-RPDOC-005-01 (Agence Nationale de la Recherche) and FRM-AJE201112 (Fondation pour la Recherche Médicale) and the Mairie de Paris Emergence Program to J. Dumont; grants NIH-R01-GM105775 and NIH-R01-AG045842 (National Institutes of Health) to M. Shirasu-Hiza; and grant NIH-DP2-OD008773 (National Institutes of Health) to J.C. Canman.

The authors declare no competing financial interests.

Author contributions: All experiments were conceived by J.C. Canman and S.N. Jordan with input from J. Dumont, T. Davies, M. Shira-

su-Hiza, and Y. Zhuravlev. S.N. Jordan did all experiments unless noted otherwise. J.C. Canman and S.N. Jordan made novel strains used in this study. T. Davies and Y. Zhuravlev did some of the PKC-3 and PAR-1/-4 experiments. J.C. Canman, S.N. Jordan, M. Shirasu-Hiza, and J. Dumont wrote the manuscript.

Submitted: 15 October 2015
Accepted: 4 December 2015

References

Audhya, A., F. Hyndman, I.X. McLeod, A.S. Maddox, J.R. Yates III, A. Desai, and K. Oegema. 2005. A complex containing the Sm protein CAR-1 and the RNA helicase CGH-1 is required for embryonic cytokinesis in *Caenorhabditis elegans*. *J. Cell Biol.* 171:267–279. http://dx.doi.org/10.1083/jcb.200506124

Audhya, A., A. Desai, and K. Oegema. 2007. A role for Rab5 in structuring the endoplasmic reticulum. *J. Cell Biol.* 178:43–56. http://dx.doi.org/10.1083/jcb.200701139

Bossinger, O., and C.R. Cowan. 2012. Methods in cell biology: Analysis of cell polarity in *C. elegans* embryos. *Methods Cell Biol.* 107:207–238. http://dx.doi.org/10.1016/B978-0-12-394620-1.00007-2

Boyd, L., S. Guo, D. Levitan, D.T. Stinchcomb, and K.J. Kemphues. 1996. PAR-2 is asymmetrically distributed and promotes association of P granules and PAR-1 with the cortex in *C. elegans* embryos. *Development.* 122:3075–3084.

Brenner, S. 1974. The genetics of *Caenorhabditis elegans*. *Genetics.* 77:71–94.

Bridges, A.A., and A.S. Gladfelter. 2015. Septin form and function at the cell cortex. *J. Biol. Chem.* 290:17173–17180. http://dx.doi.org/10.1074/jbc.R114.634444

Burkel, B.M., G. von Dassow, and W.M. Bement. 2007. Versatile fluorescent probes for actin filaments based on the actin-binding domain of utrophin. *Cell Motil. Cytoskeleton.* 64:822–832. http://dx.doi.org/10.1002/cm.20226

Cabernard, C., K.E. Prehoda, and C.Q. Doe. 2010. A spindle-independent cleavage furrow positioning pathway. *Nature.* 467:91–94. http://dx.doi.org/10.1038/nature09334

Chang, F., A. Woollard, and P. Nurse. 1996. Isolation and characterization of fission yeast mutants defective in the assembly and placement of the contractile actin ring. *J. Cell Sci.* 109:131–142.

Chartier, N.T., D.P. Salazar Ospina, L. Benkemoun, M. Mayer, S.W. Grill, A.S. Maddox, and J.C. Labbé. 2011. PAR-4/LKB1 mobilizes nonmuscle myosin through anillin to regulate *C. elegans* embryonic polarization and cytokinesis. *Curr. Biol.* 21:259–269. http://dx.doi.org/10.1016/j.cub.2011.01.010

Cheeks, R.J., J.C. Canman, W.N. Gabriel, N. Meyer, S. Strome, and B. Goldstein. 2004. *C. elegans* PAR proteins function by mobilizing and stabilizing asymmetrically localized protein complexes. *Curr. Biol.* 14:851–862. http://dx.doi.org/10.1016/j.cub.2004.05.022

Cuenca, A.A., A. Schetter, D. Aceto, K. Kemphues, and G. Seydoux. 2003. Polarization of the *C. elegans* zygote proceeds via distinct establishment and maintenance phases. *Development.* 130:1255–1265. http://dx.doi.org/10.1242/dev.00284

Davies, T., S.N. Jordan, V. Chand, J.A. Sees, K. Laband, A.X. Carvalho, M. Shirasu-Hiza, D.R. Kovar, J. Dumont, and J.C. Canman. 2014. High-resolution temporal analysis reveals a functional timeline for the molecular regulation of cytokinesis. *Dev. Cell.* 30:209–223. http://dx.doi.org/10.1016/j.devcel.2014.05.009

Davoli, T., and T. de Lange. 2011. The causes and consequences of polyploidy in normal development and cancer. *Annu. Rev. Cell Dev. Biol.* 27:585–610. http://dx.doi.org/10.1146/annurev-cellbio-092910-154234

Dechant, R., and M. Glotzer. 2003. Centrosome separation and central spindle assembly act in redundant pathways that regulate microtubule density and trigger cleavage furrow formation. *Dev. Cell.* 4:333–344. http://dx.doi.org/10.1016/S1534-5807(03)00057-1

Field, C.M., M. Coughlin, S. Doberstein, T. Marty, and W. Sullivan. 2005. Characterization of anillin mutants reveals essential roles in septin localization and plasma membrane integrity. *Development.* 132:2849–2860. http://dx.doi.org/10.1242/dev.01843

Field, C.M., A.S. Maddox, J.R. Pringle, and K. Oegema. 2008. Septins in the metazoan model systems *Drosophila melanogaster* and *Caenorhabditis elegans*. The Septins. P.A. Hall, S.E.H. Russell, and J.R. Pringle, editors. John Wiley and Sons, Ltd, Chichester, UK. 147–168.

Fievet, B.T., J. Rodriguez, S. Naganathan, C. Lee, E. Zeiser, T. Ishidate, M. Shirayama, S. Grill, and J. Ahringer. 2013. Systematic genetic interaction screens uncover cell polarity regulators and functional redundancy. *Nat. Cell Biol.* 15:103–112. http://dx.doi.org/10.1038/ncb2639

Ganem, N.J., Z. Storchova, and D. Pellman. 2007. Tetraploidy, aneuploidy and cancer. *Curr. Opin. Genet. Dev.* 17:157–162. http://dx.doi.org/10.1016/j.gde.2007.02.011

Gönczy, P., H. Schnabel, T. Kaletta, A.D. Amores, T. Hyman, and R. Schnabel. 1999. Dissection of cell division processes in the one cell stage *Caenorhabditis elegans* embryo by mutational analysis. *J. Cell Biol.* 144:927–946. http://dx.doi.org/10.1083/jcb.144.5.927

Green, R.A., E. Paluch, and K. Oegema. 2012. Cytokinesis in animal cells. *Annu. Rev. Cell Dev. Biol.* 28:29–58. http://dx.doi.org/10.1146/annurev-cellbio-101011-155718

Guo, S., and K.J. Kemphues. 1996. A non-muscle myosin required for embryonic polarity in *Caenorhabditis elegans*. *Nature.* 382:455–458. http://dx.doi.org/10.1038/382455a0

Halaoui, R., and L. McCaffrey. 2015. Rewiring cell polarity signaling in cancer. *Oncogene.* 34:939–950. http://dx.doi.org/10.1038/onc.2014.59

Hird, S.N., and J.G. White. 1993. Cortical and cytoplasmic flow polarity in early embryonic cells of *Caenorhabditis elegans*. *J. Cell Biol.* 121:1343–1355. http://dx.doi.org/10.1083/jcb.121.6.1343

Hoege, C., and A.A. Hyman. 2013. Principles of PAR polarity in *Caenorhabditis elegans* embryos. *Nat. Rev. Mol. Cell Biol.* 14:315–322. http://dx.doi.org/10.1038/nrm3558

Kamath, R.S., and J. Ahringer. 2003. Genome-wide RNAi screening in *Caenorhabditis elegans*. *Methods.* 30:313–321. http://dx.doi.org/10.1016/S1046-2023(03)00050-1

Kemphues, K.J., J.R. Priess, D.G. Morton, and N.S. Cheng. 1988. Identification of genes required for cytoplasmic localization in early *C. elegans* embryos. *Cell.* 52:311–320. http://dx.doi.org/10.1016/S0092-8674(88)80024-2

Lacroix, B., and A.S. Maddox. 2012. Cytokinesis, ploidy and aneuploidy. *J. Pathol.* 226:338–351. http://dx.doi.org/10.1002/path.3013

Lewellyn, L., J. Dumont, A. Desai, and K. Oegema. 2010. Analyzing the effects of delaying aster separation on furrow formation during cytokinesis in the *Caenorhabditis elegans* embryo. *Mol. Biol. Cell.* 21:50–62. http://dx.doi.org/10.1091/mbc.E09-01-0089

Lewellyn, L., A. Carvalho, A. Desai, A.S. Maddox, and K. Oegema. 2011. The chromosomal passenger complex and centralspindlin independently contribute to contractile ring assembly. *J. Cell Biol.* 193:155–169. http://dx.doi.org/10.1083/jcb.201008138

Liu, J., L.L. Maduzia, M. Shirayama, and C.C. Mello. 2010. NMY-2 maintains cellular asymmetry and cell boundaries, and promotes a SRC-dependent asymmetric cell division. *Dev. Biol.* 339:366–373. http://dx.doi.org/10.1016/j.ydbio.2009.12.041

Macara, I.G. 2004. Par proteins: partners in polarization. *Curr. Biol.* 14:R160–R162. http://dx.doi.org/10.1016/j.cub.2004.01.048

Maddox, A.S., L. Lewellyn, A. Desai, and K. Oegema. 2007. Anillin and the septins promote asymmetric ingression of the cytokinetic furrow. *Dev. Cell.* 12:827–835. http://dx.doi.org/10.1016/j.devcel.2007.02.018

Menon, M.B., and M. Gaestel. 2015. Sep(t)arate or not – how some cells take septin-independent routes through cytokinesis. *J. Cell Sci.* 128:1877–1886. http://dx.doi.org/10.1242/jcs.164830

Motegi, F., and G. Seydoux. 2013. The PAR network: redundancy and robustness in a symmetry-breaking system. *Philos. Trans. R. Soc. Lond. B Biol. Sci.* 368:20130010. http://dx.doi.org/10.1098/rstb.2013.0010

Munro, E., J. Nance, and J.R. Priess. 2004. Cortical flows powered by asymmetrical contraction transport PAR proteins to establish and maintain anterior-posterior polarity in the early *C. elegans* embryo. *Dev. Cell.* 7:413–424. http://dx.doi.org/10.1016/j.devcel.2004.08.001

Nguyen, T.Q., H. Sawa, H. Okano, and J.G. White. 2000. The *C. elegans* septin genes, unc-59 and unc-61, are required for normal postembryonic cytokineses and morphogenesis but have no essential function in embryogenesis. *J. Cell Sci.* 113:3825–3837.

Norden, C., M. Mendoza, J. Dobbelaere, C.V. Kotwaliwale, S. Biggins, and Y. Barral. 2006. The NoCut pathway links completion of cytokinesis to spindle midzone function to prevent chromosome breakage. *Cell.* 125:85–98. http://dx.doi.org/10.1016/j.cell.2006.01.045

O'Farrell, F., and P. Kylsten. 2008. *Drosophila* Anillin is unequally required during asymmetric cell divisions of the PNS. *Biochem. Biophys. Res. Commun.* 369:407–413. http://dx.doi.org/10.1016/j.bbrc.2008.02.060

Oegema, K., M.S. Savoian, T.J. Mitchison, and C.M. Field. 2000. Functional analysis of a human homologue of the *Drosophila* actin binding protein anillin suggests a role in cytokinesis. *J. Cell Biol.* 150:539–552. http://dx.doi.org/10.1083/jcb.150.3.539

Pacquelet, A., P. Uhart, J.P. Tassan, and G. Michaux. 2015. PAR-4 and anillin regulate myosin to coordinate spindle and furrow position during asymmetric division. *J. Cell Biol.* 210:1085–1099. http://dx.doi.org/10.1083/jcb.201503006

Paolini, A., A.L. Duchemin, S. Albadri, E. Patzel, D. Bornhorst, P. González Avalos, S. Lemke, A. Machate, M. Brand, S. Sel, et al. 2015. Asymmetric inheritance of the apical domain and self-renewal of retinal ganglion cell progenitors depend on Anillin function. *Development.* 142:832–839. http://dx.doi.org/10.1242/dev.118612

Piekny, A.J., and M. Glotzer. 2008. Anillin is a scaffold protein that links RhoA, actin, and myosin during cytokinesis. *Curr. Biol.* 18:30–36. http://dx.doi.org/10.1016/j.cub.2007.11.068

Pittman, K.J., and A.R. Skop. 2012. Anterior PAR proteins function during cytokinesis and maintain DYN-1 at the cleavage furrow in *Caenorhabditis elegans*. *Cytoskeleton (Hoboken).* 69:826–839. http://dx.doi.org/10.1002/cm.21053

Rose, L., and P. Gönczy. 2014. Polarity establishment, asymmetric division and segregation of fate determinants in early *C. elegans* embryos. *WormBook.* http://dx.doi.org/10.1895/wormbook.1.30.2

Schenk, C., H. Bringmann, A.A. Hyman, and C.R. Cowan. 2010. Cortical domain correction repositions the polarity boundary to match the cytokinesis furrow in *C. elegans* embryos. *Development.* 137:1743–1753. http://dx.doi.org/10.1242/dev.040436

Schonegg, S., A.T. Constantinescu, C. Hoege, and A.A. Hyman. 2007. The Rho GTPase-activating proteins RGA-3 and RGA-4 are required to set the initial size of PAR domains in *Caenorhabditis elegans* one-cell embryos. *Proc. Natl. Acad. Sci. USA.* 104:14976–14981. http://dx.doi.org/10.1073/pnas.0706941104

Severson, A.F., D.L. Baillie, and B. Bowerman. 2002. A formin homology protein and a profilin are required for cytokinesis and Arp2/3-independent assembly of cortical microfilaments in *C. elegans*. *Curr. Biol.* 12:2066–2075. http://dx.doi.org/10.1016/S0960-9822(02)01355-6

Shelton, C.A., J.C. Carter, G.C. Ellis, and B. Bowerman. 1999. The nonmuscle myosin regulatory light chain gene *mlc-4* is required for cytokinesis, anterior-posterior polarity, and body morphology during *Caenorhabditis elegans* embryogenesis. *J. Cell Biol.* 146:439–451. http://dx.doi.org/10.1083/jcb.146.2.439

Straight, A.F., C.M. Field, and T.J. Mitchison. 2005. Anillin binds nonmuscle myosin II and regulates the contractile ring. *Mol. Biol. Cell.* 16:193–201. http://dx.doi.org/10.1091/mbc.E04-08-0758

Suzuki, A., and S. Ohno. 2006. The PAR-aPKC system: lessons in polarity. *J. Cell Sci.* 119:979–987. http://dx.doi.org/10.1242/jcs.02898

Swan, K.A., A.F. Severson, J.C. Carter, P.R. Martin, H. Schnabel, R. Schnabel, and B. Bowerman. 1998. cyk-1: a *C. elegans* FH gene required for a late step in embryonic cytokinesis. *J. Cell Sci.* 111:2017–2027.

Timmons, L., D.L. Court, and A. Fire. 2001. Ingestion of bacterially expressed dsRNAs can produce specific and potent genetic interference in *Caenorhabditis elegans*. *Gene.* 263:103–112. http://dx.doi.org/10.1016/S0378-1119(00)00579-5

Tormos, A.M., R. Taléns-Visconti, and J. Sastre. 2015. Regulation of cytokinesis and its clinical significance. *Crit. Rev. Clin. Lab. Sci.* 52:159–167.

Tse, Y.C., M. Werner, K.M. Longhini, J.C. Labbe, B. Goldstein, and M. Glotzer. 2012. RhoA activation during polarization and cytokinesis of the early *Caenorhabditis elegans* embryo is differentially dependent on NOP-1 and CYK-4. *Mol. Biol. Cell.* 23:4020–4031. http://dx.doi.org/10.1091/mbc.E12-04-0268

Velarde, N., K.C. Gunsalus, and F. Piano. 2007. Diverse roles of actin in *C. elegans* early embryogenesis. *BMC Dev. Biol.* 7:142. http://dx.doi.org/10.1186/1471-213X-7-142

Verbrugghe, K.J., and J.G. White. 2007. Cortical centralspindlin and Gα have parallel roles in furrow initiation in early *C. elegans* embryos. *J. Cell Sci.* 120:1772–1778. http://dx.doi.org/10.1242/jcs.03447

Watts, J.L., D.G. Morton, J. Bestman, and K.J. Kemphues. 2000. The *C. elegans* par-4 gene encodes a putative serine-threonine kinase required for establishing embryonic asymmetry. *Development.* 127:1467–1475.

Williams, S.E., and E. Fuchs. 2013. Oriented divisions, fate decisions. *Curr. Opin. Cell Biol.* 25:749–758. http://dx.doi.org/10.1016/j.ceb.2013.08.003

Wloka, C., R. Nishihama, M. Onishi, Y. Oh, J. Hanna, J.R. Pringle, M. Krauss, and E. Bi. 2011. Evidence that a septin diffusion barrier is dispensable for cytokinesis in budding yeast. *Biol. Chem.* 392:813–829. http://dx.doi.org/10.1515/BC.2011.083

Wu, J.Q., Y. Ye, N. Wang, T.D. Pollard, and J.R. Pringle. 2010. Cooperation between the septins and the actomyosin ring and role of a cell-integrity pathway during cell division in fission yeast. *Genetics.* 186:897–915. http://dx.doi.org/10.1534/genetics.110.119842

Jordan et al., http://www.jcb.org/cgi/content/full/jcb.201510063/DC1

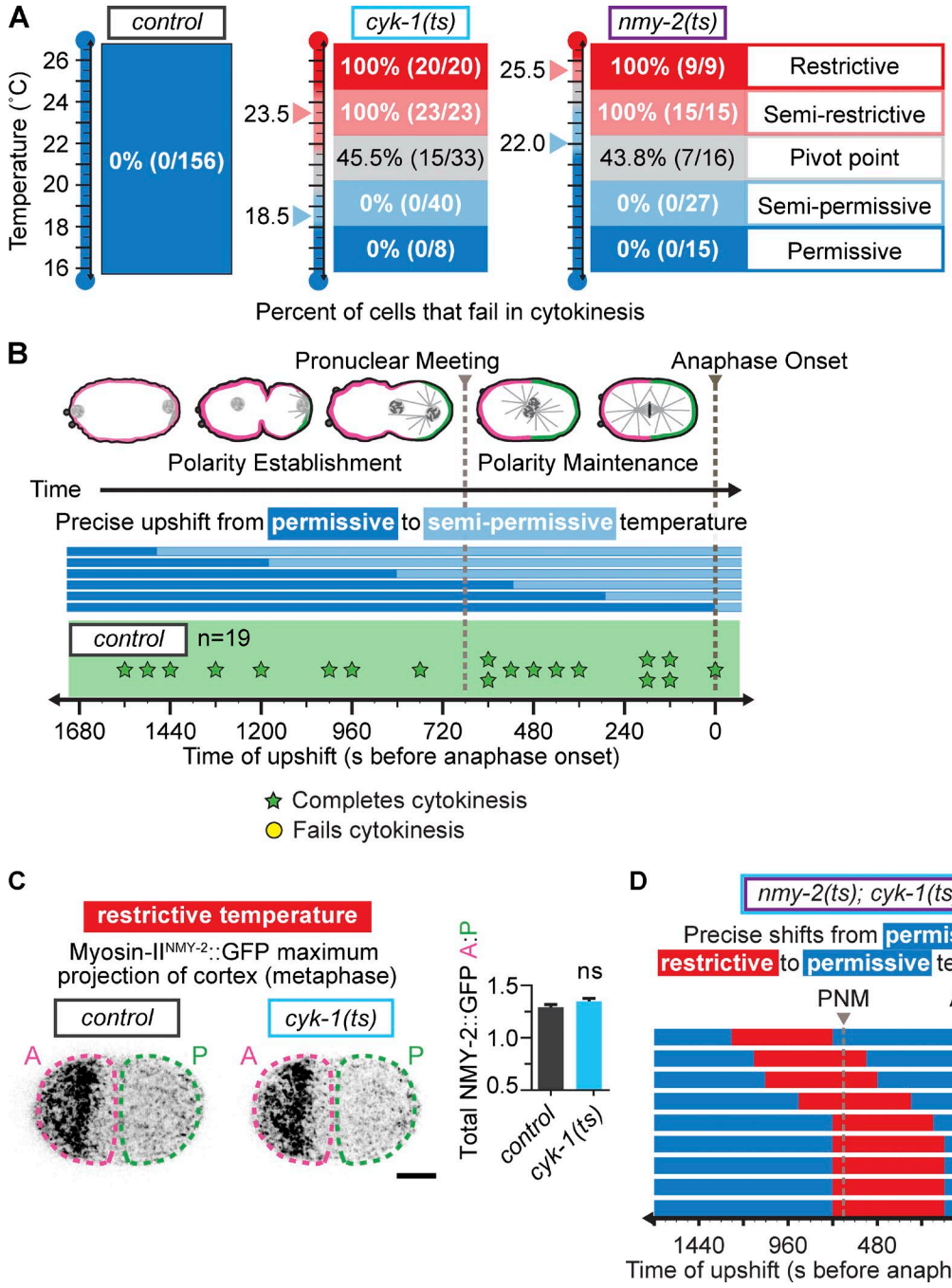

Figure S1. **ts mutants allow tuning of specific protein functions that are necessary for cytokinesis.** (A) Temperature response tables for control, *formin(ts)*, and *myosin-II(ts)* embryos. Formin and myosin-II fast-acting ts mutants have tunable constriction defects dependent on temperature. (B) Control embryos complete cytokinesis when upshifted to a semipermissive temperature before cytokinesis. (C) At fully restrictive temperature, *formin(ts)* embryos successfully polarize myosin-II (NMY-2::GFP) in an anterior cap before cytokinesis. ns, not significant. Error bars represent SD. (D) Double *myosin-II(ts);formin(ts)* mutant embryos complete cytokinesis when temporarily upshifted to restrictive temperature and returned to a fully permissive temperature before anaphase onset (AO), indicating that these ts mutant phenotypes are reversible. PNM, pronuclear meeting. Bar, 10 µm. *cyk-1* = *formin*; *nmy-2* = *myosin-II*.

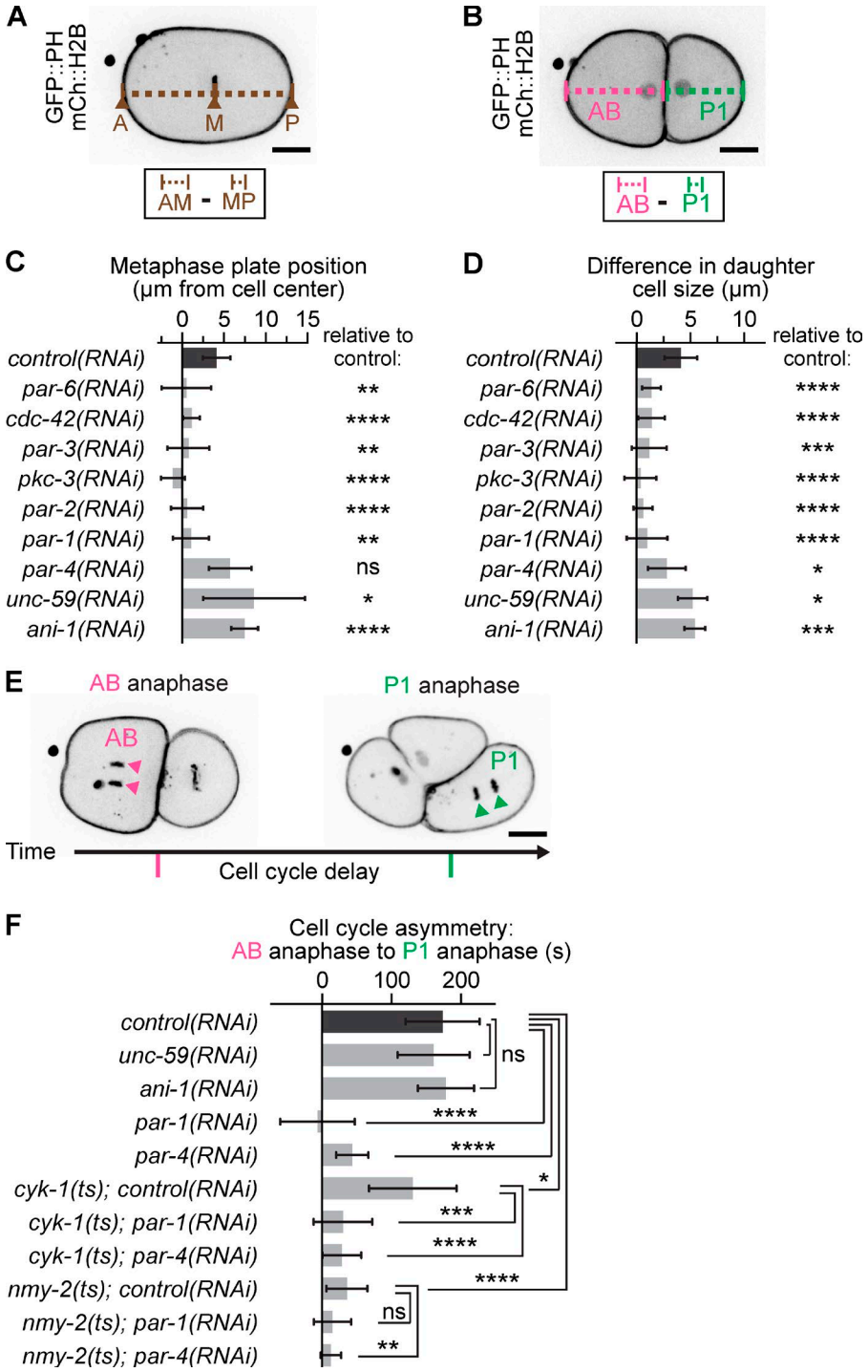

Figure S2. **Successful RNAi-mediated knockdown of PAR proteins was confirmed using hallmarks of the loss of polarity.** (A) Metaphase plate (m) position in RNAi-depleted embryos was measured immediately before anaphase onset by calculating the deviation in position of the metaphase plate from the cell center (at 0 µm) toward the anterior (negative change) or posterior (positive change). (B) Daughter cell size asymmetry was measured immediately after contractile ring closure. Asymmetric division is indicated by an increased difference in daughter cell length (when AB > P1). (C) Metaphase plate position for RNAi-depleted embryos. (D) Daughter cell size asymmetry for RNAi-depleted embryos. (E) Successful depletion of cytoplasmic polarity regulators (PAR-1 and PAR-4) was determined by measuring the loss of the cell cycle delay between anaphase onset in the AB blastomere and anaphase onset in the P1 blastomere. In control embryos, there is a significant delay between the two cell cycles; this difference is lost upon disruption of cytoplasmic polarity. (F) Difference in time between anaphase of AB and anaphase of P1. All data are shown as mean ± SD. *, $P < 0.05$; **, $P < 0.005$; ***, $P < 0.0005$; ****, $P < 0.0001$; ns, not significant. Bars, 10 µm. *cyk-1 = formin; nmy-2 = myosin-II; unc-59 = septin; ani-1 = anillin.*

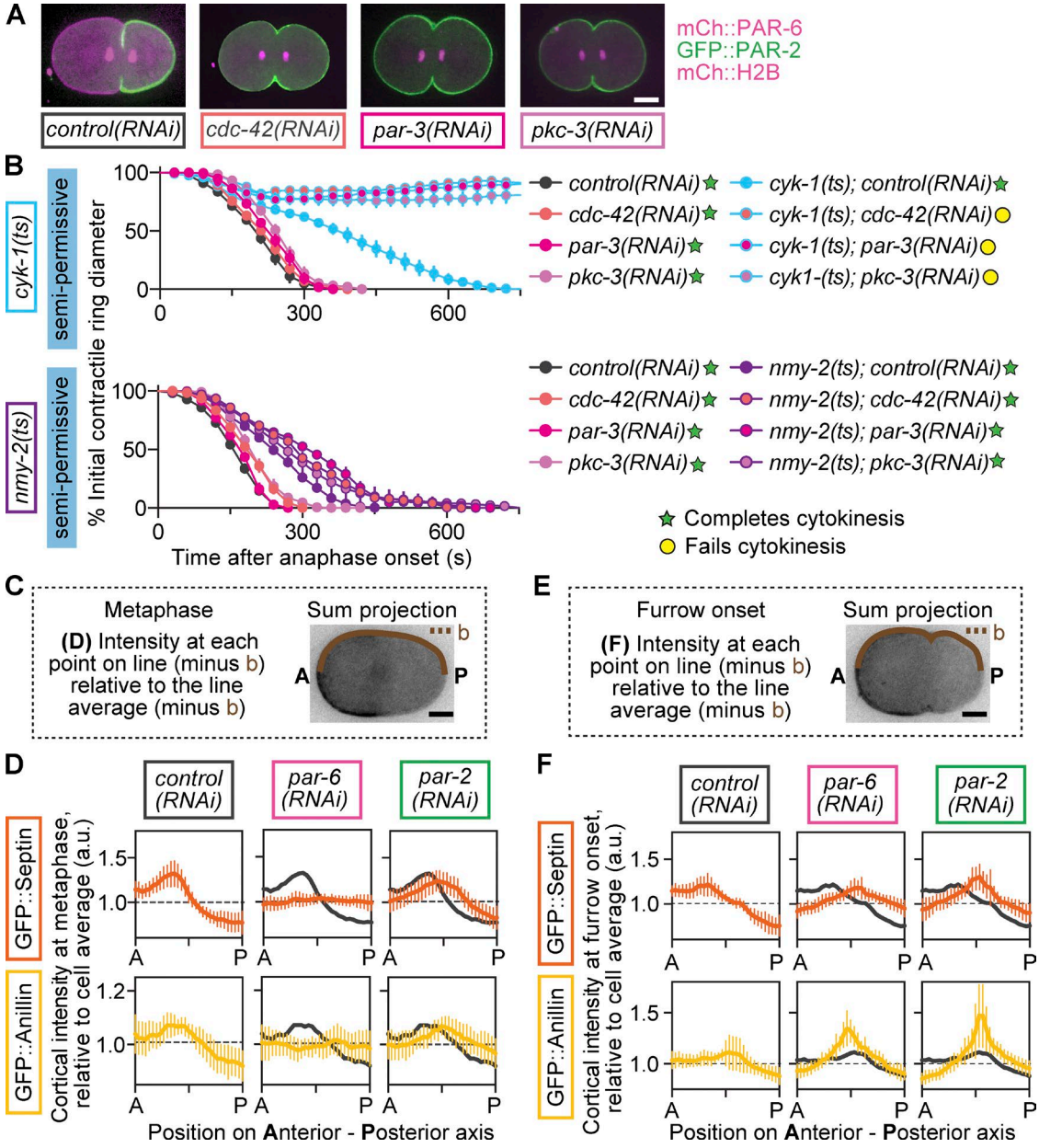

Figure S3. **Cortical PAR proteins regulate cytokinesis and sequester septin and anillin in the cell anterior.** (A) Depletion of the aPAR proteins CDC-42, PAR-3, and PKC-3 results in an expansion of the pPAR protein PAR-2 into the entire cell cortex. (B) RNAi-mediated depletion of cortical aPAR proteins (CDC-42, PAR-3, or PKC-3) leads to cytokinesis failure in *formin(ts)* but not *myosin-II(ts)* mutant embryos at semipermissive temperature ($n \geq 9$, all conditions; mean ± SEM). (C) Schematic of line scan taken for quantifications in D to measure reporter localization. (D) At metaphase, septin and anillin are enriched in the cell anterior in a PAR-dependent manner ($n \geq 10$, all conditions; mean ± SD). (E) Schematic of line scan taken for quantifications in F to quantify reporter localization. (F) At furrow onset, septin and anillin are enriched in the cell anterior in a PAR-dependent manner ($n \geq 10$, all conditions; mean ± SD). (D and F) Mean from *control(RNAi)* is displayed for reference. Bars, 10 µm. a.u., arbitrary units; b, background. *cyk-1* = *formin*; *nmy-2* = *myosin-II*.

Table S1. **Strain names and genotypes**

Strain	Genotype
OD95	*unc-119(ed3)*[a] *ltIs38 [pAA1; pie-1/GFP::PH(PLC1delta1); unc-119 (+)]III; ltIs37 [pAA64; pie-1/mCHERRY::his-58; unc-119(+)]IV*
JCC146	*cyk-1(or596ts) unc-119(ed3)*[a] *ltIs38 [pAA1; pie-1/GFP::PH(PLC1delta1); unc-119(+)]III; ltIs37 [pAA64; pie-1/mCHERRY::his-58; unc-119(+)]IV*
JCC192	*nmy-2(ne3409ts) dpy-5*[b] *I; unc-119(ed3)*[a] *ltIs38 [pAA1; pie-1/GFP::PH(PLC1delta1); unc-119(+)]III; ltIs37 [pAA64; pie-1/mCHERRY::his-58; unc-119(+)]IV*
JCC212	*nmy-2(ne3409ts) dpy-5*[b] *I; cyk-1(or596ts) unc-119(ed3)*[a] *ltIs38 [pAA1; pie-1/GFP::PH(PLC1delta1); unc-119(+)]III; ltIs37 [pAA64; pie-1/mCHERRY::his-58; unc-119(+)]IV*
JCC744	*unc-119(ed3)*[a] *III; ddIs25 [GFP::F58B6.3;unc-119(+)]; ddIs26 [mCherry::T26E3.3;unc-119(+)]; ltIs37 [pAA64; pie-1/mCHERRY::his-58; unc-119(+)]IV*
JCC719	*mgSi3[cb-unc-119(+); GFP:UTROPHIN]II; unc-119(ed3)*[a] *III; ltIs37 [pAA64; pie-1/mCHERRY::his-58; unc-119(+)]IV*
JCC541	*unc-119(ed3)*[a] *III; ltIs37 [pAA64; pie-1/mCHERRY::his-58; unc-119 (+)] IV; zuIs45[nmy-2::NMY-2::GFP; unc-119(+)]V*
JCC559	*cyk-1(or596ts) unc-119(ed3)*[a] *III; ltIs37 [pAA64; pie-1/mCHERRY::his-58; unc-119(+)] IV; zuIs45[nmy-2::NMY-2::GFP; unc-119(+)] V*
JCC425	*unc-119(ed3)*[a] *III; ltIs37 [pAA64; pie-1/mCHERRY::his-58; unc-119(+)] IV; ltIs20 [pASM10; pie-1:GFP::unc-59; unc-119(+)]*
OD159	*unc-119(ed3)*[a] *III; ltIs86 [pASM65; pie-1:ani-1(fl cDNA)::GFP; unc-119(+)]*

[a]The unc-119(ed3) mutation was present in the parental strains but has not been directly sequenced in these strains to determine if the unc-119 gene is mutated.
[b]The exact dpy-5 allele is unknown but presumed to be e61, as published in Carvalho et al. (2009).

Table S2. **Feeding RNAi constructs**

Plasmid	Gene(s)	Oligo 1 (5′-3′)	Oligo 2 (5′-3′)	Template	Cloning Vector
pJC165	*par-1* (*H39E23.1*)	gcgcgACTAGTttgctgattttggattttcg	gcgcgACTAGTgctgatcctgcagtgattgat	N2 cDNA	L4440 (empty vector)
pJC317	*par-2* (*F58B6.3*)	gcgcgACTAGTcggccgctctagaactagtat	gcgcgACTAGTtcctgcagcccgggggat	N2 cDNA	L4440
pJC166	*pkc-3* (*F09E5.1*)	gcgcgACTAGTcgtctccgacatcattagagg	gcgcgACTAGTgattcggtctggaagcaaga	N2 cDNA	L4440
pJC186	*par-4* (*Y59A8B.14*)	gcgcgACTAGTgggccgtcaaaattatgaaat	gcgcgACTAGTaggccttgatcctctggg	N2 cDNA	L4440
pJC132	*ani-1* (*Y49E10.19*)	gcgcgACTAGTactccagtgcattttcaccc	gcgcgACTAGTgacgatgatgatgatgtcgc	N2 cDNA	L4440
pJC43	*par-3* (*F54E7.3*)	Acquired from Ahringer library (Clone # III-3A01)			
pJC56	*par-6* (*T26E3.3*)	Acquired from Ahringer library (Clone # I-6M10)			
pJC53	*cdc-42* (*R07G3.1*)	Acquired from Ahringer library (Clone # II-5P13)			
pJC55	*unc-59* (*W09C5.2*)	Acquired from Ahringer library (Clone # I-6N04)			
pJC319	*par-2* (*F58B6.3*) and *unc-59* (*W09C5.2*)	gcgcgGAATTCcggccgctctagaactagtat	gcgcgGAATTCtcctgcagcccgggggat	pJC317 (par-2)	pJC55 (unc-59)
pJC318	*par-6* (*T26E3.3*) and *unc-59* (*W09C5.2*)	gcgcgGAATTCgaaaaatccaaattttca	gcgcgGAATTCttaacgatttttgagctgt	pJC56 (par-6)	pJC55 (unc-59)

This table details the feeding RNAi constructs used in this study, including plasmid names, targeted genes for RNAi experiments, oligos used to generate RNAi feeding construct and DNA template used or Ahringer library (Kamath and Ahringer, 2003; Kamath et al., 2003) clone number, and cloning vectors used in this study.

References

Carvalho, A., A. Desai, and K. Oegema. 2009. Structural memory in the contractile ring makes the duration of cytokinesis independent of cell size. *Cell*. 926–937. http://dx.doi.org/10.1016/j.cell.2009.03.021

Kamath, R.S., and J. Ahringer. 2003. Genome-wide RNAi screening in *Caenorhabditis elegans*. *Methods.* 30:313–321. http://dx.doi.org/10.1016/S1046-2023(03)00050-1

Kamath, R.S., A.G. Fraser, Y. Dong, G. Poulin, R. Durbin, M. Gotta, A. Kanapin, N. Le Bot, S. Moreno, M. Sohrmann, et al. 2003. Systematic functional analysis of the *Caenorhabditis elegans* genome using RNAi. *Nature.* 421:231–237. http://dx.doi.org/10.1038/nature01278